Synthesis, Characterization, and Bonding of Indium Clusters: $A_3Na_{26}In_{48}$ (A = K, Rb, Cs) with a Novel Cubic Network of *arachno*- and *closo*-In_{12} Clusters

Slavi C. Sevov and John D. Corbett*

Department of Chemistry and Ames Laboratory—DOE,[1] Iowa State University, Ames, Iowa 50011

Received October 20, 1992

The title compounds are obtained in high yield by slow cooling of the appropriate fused mixture of elements in welded Ta. They occur in the cubic space group $Pm\bar{3}n$, $Z = 2$, with $a = 16.0640(4)$, 16.101(1), 16.130(1) Å for A = K, Rb, Cs, respectively. The structure was refined by single-crystal means for A = K, Rb to R, R_w = 2.5, 3.3 and 2.0, 2.5%. The structure contains *closo*-In_{12} icosahedra (T_h symmetry) plus *arachno*-In_{12} (D_{2d}) as approximate (D_{6d}) hexagonal antiprisms (drums) with 12 exo In–In bonds about each cluster. Nonintersecting chains of "drums" lie in the faces of the cubic cell and parallel to the cell edges. Adjacent arachno clusters are interconnected only indirectly at chain crossings via the closo polyhedra that define a body-centered cube. The structure is A15 (Cr_3Si)-like with *arachno*- and *closo*-In_{12} clusters, respectively, replacing the metal and non-metal atoms of the parent. The larger A cations order in, and appear required for, the larger cavities lying betwen drums in each chain. The compounds are electron-rich by 5.5% according to theory, and the potassium example is metallic ($\rho_{295} \sim 23$ μΩ cm) and Pauli paramagnetic (2.2×10^{-3} emu mol^{-1}) by measurement.

Introduction

Even the binary compounds in the alkali metal–gallium[2-4] and –indium[5-10] systems are remarkable in their structural novelty and complexity. The most striking lesson to be gained from these is the very considerable driving force shown by these post-transition "metallic" elements in negative oxidation states to localize electrons in covalent bonds and the fascinating variety of ways this can be accomplished. The generic shortage of electrons with these elements means that either large negative charges or delocalized bonding (or both) will pertain. Characteristically, the delocalized versions feature either familiar or new varieties of naked clusters. A few isolated and hypoelectronic clusters are found for indium,[5,7] while the alternative linkage of clusters into networks via simple exo bonds is frequently observed for both elements. The networks may be remarkably complex and diverse in response to an evident parallel tendency to achieve bonding situations that are close to valence (Zintl) phases. For example, we have earlier completed a study of the entire Na–In system and found that it contains four phases: $Na_{15}In_{27.4}$ with interconnected *closo*-In_{16}, *nido*-In_{11}, *arachno*-In_{10}, and four-bonded In units;[7] $Na_7In_{11.8}$ with somewhat related cluster units in a different network;[6] the traditional Zintl phase NaIn with a diamond-like anionic array;[11] and Na_2In with isolated tetrahedra.[7] The second phase is especially noteworthy in that it comes within 0.6% of being electron-precise. It is also noteworthy that the K–In system contains four completely different phases.[5,10]

The subtle but important effects of cation size and number suggest that mixed cations may produce yet other arrangements. Such have already been observed for gallium,[12] but it also seems likely that the differences between gallium and indium structures in this sort of chemistry may be greater than their similarities. Three phases are found in the K_8In_{11}–$Na_7In_{11.8}$ pseudobinary system, and this article reports on the most distinctive of these, the cubic $K_3Na_{26}In_{48}$ and its analogues with other cations in place of potassium.

Experimental Section

Synthesis. All materials were handled in a N_2-filled glovebox that had a typical H_2O level of <0.1 ppm vol. The surfaces of the indium (Cerac, 99.999%), sodium (Alfa, 99.9+%, sealed under Ar), and potassium (J. T. Baker, lump under oil, purified 98+%) were cut clean with a scalpel before use. The potassium lump was washed with hexane and dried under vacuum before introduction into the glovebox. Rubidium (Alfa, 99.9%, sealed under Ar) and cesium (Alfa, 99.98%, sealed under Ar) were used as received, the amounts loaded being weighed by difference. (Loss of alkali metal on transfer is the most probable error.) All reactions were carried out in welded tantalum tubes jacketed in sealed SiO_2 containers. The techniques are described elsewhere.[6,7]

Samples with atomic ratios of K:Na:In = 1:7:11, Rb:Na:In = 2:6:11, and Cs:Na:In = 3:26:48 were prepared, and the mixtures were melted at 550 °C for 10 h. (The highest melting points in the Na–In, K–In, and Rb–In systems are about 441, 478, and 522 °C, respectively.[13]) The samples were then slowly cooled to room temperature at 3 °C/h. The products had gray metallic appearances and were very brittle.

Powder patterns were obtained from ground samples that were mounted between pieces of cellophane tape. An Enraf-Nonius Guinier camera, Cu Kα radiation (λ = 1.540 562 Å), and NBS (NIST) silicon as internal standard were employed for this purpose. X-ray powder patterns calculated on the basis of the refined positional parameters for A = K (below) matched the respective ones measured for the Rb–Na–In and Cs–Na–In products very well, leading to the conclusion that the same structure pertained to all three. (That for Rb showed ~15–20% of Rb_2In_3[8] as a second phase.) A least-squares refinement of the measured 2θ values together with those of the standard Si lines resulted in $a = 16.0640(4)$ Å for $K_3Na_{26}In_{48}$, $a = 16.101(1)$ Å, for $Rb_3Na_{26}In_{48}$, and $a = 16.130(1)$ Å for $Cs_3Na_{26}In_{48}$. All the patterns also contained weak lines for indium metal, probably from adventitious oxidation or hydrolysis of the very sensitive samples during the X-ray exposure.

Structure Determination. Diffraction data for $K_3Na_{26}In_{48}$ and $Rb_3Na_{26}In_{48}$ were collected on a CAD4 single-crystal diffractometer at 21 °C with monochromated Mo Kα radiation up to $2\theta = 50°$. The structures were refined with the aid of the TEXSAN package. Some details of the data collection and refinement for the two structures are listed in Table I. Unique aspects of the crystallography follow:

(1) Ames Laboratory is operated for the Department of Energy by Iowa State University under Contract No. W-7405-Eng-82. This research was supported by the U.S. Department of Energy, Office of Basic Energy Sciences, Materials Sciences Division.
(2) Belin, C.; Tillard-Charbonnel, M. *Prog. Solid State Chem.* **1993**, *22*, 59.
(3) Schäfer, H. *J. Solid State Chem.* **1985**, *57*, 97.
(4) Burdett, J. K.; Canadell, E. *J. Am. Chem. Soc.* **1990**, *112*, 7207.
(5) Sevov, S. C.; Corbett, J. D. *Inorg. Chem.* **1991**, *30*, 4875.
(6) Sevov, S. C.; Corbett, J. D. *Inorg. Chem.* **1992**, *31*, 1895.
(7) Sevov, S. C.; Corbett, J. D. *J. Solid State Chem.*, in press.
(8) Sevov, S. C.; Corbett, J. D. *Z. Anorg. Allg. Chem.* **1993**, *619*, 128.
(9) Sevov, S. C.; Corbett, J. D. *Inorg. Chem.* **1993**, *32*, 1059.
(10) Sevov, S. C.; Corbett, J. D. Unpublished research.
(11) Zintl, E.; Neumayr, S. *Z. Phys. Chem.* **1933**, *B20*, 270.
(12) Belin, C.; Charbonnel, M. *J. Solid State Chem.* **1986**, *64*, 57.
(13) *Binary Alloy Phase Diagrams*, 2nd ed.; American Society for Metals: Metals Park, OH 44073; Vol. 3, pp 2261, 2250, and 2280, respectively.

0020-1669/93/1332-1612$04.00/0

Table I. Selected Data Collection and Refinement Parameters for $K_3Na_{26}In_{48}$ and $Rb_3Na_{26}In_{48}$

Formula	$K_3Na_{26}In_{48}$	$Rb_3Na_{26}In_{48}$
space group, Z	$Pm\bar{3}n$ (No. 223), 2	$Pm\bar{3}n$ (No. 223), 2
a,[a] Å	16.0640(4)	16.101(1)
V, Å^3	4145.3(1)	4174.1(3)
d(calc), g cm^{-3}	4.99	5.06
abs coeff (Mo Kα), cm^{-1}	131.5	146.0
transm coeff range	0.429–1.000	0.405–1.000
no. of indep obs reflns, variables	479, 39	578, 39
R, R_w,[b] %	2.5, 3.3	2.0, 2.5

[a] Room-temperature Guinier data with Si as an internal standard (λ = 1.540 562 Å). [b] $R = \Sigma||Fo| - |Fc||/\Sigma|Fo|$; $R_w = [\Sigma w(|Fo| - |Fc|)^2/\Sigma w(Fo)^2]^{1/2}$; $w = \sigma_F^{-2}$.

$K_3Na_{26}In_{48}$. A few small pieces of the crushed sample were selected, sealed in thin-walled glass capillaries, and checked for singularity by means of oscillation photographs. A platelike example, 0.1 × 0.2 × 0.2 mm, was studied by Weissenberg photography, which showed that the cell was primitive cubic with a systematic absence condition hhl ($l = 2n$) consistent with two possible space groups, $P4\bar{3}n$ and $Pm\bar{3}n$. The same crystal was mounted on the diffractometer, and reflections from a random search were indexed with a cubic cell of the expected dimension. Data from one octant of reciprocal space confirmed the two possible space groups after correction for Lorentz and polarization effects and for absorption with the aid of the average of four ψ-scans at different angles. The Wilson plot indicated a centrosymmetric distribution, and therefore $Pm\bar{3}n$ was chosen for the first trial.

Direct methods provided seven peaks, but only the first three had distances to each other appropriate for indium atoms, and they were so assigned. A few cycles of least-squares refinement and a difference Fourier synthesis revealed the last four plus one more that had A–In distances in the range seen before for A = K or Na. One had relatively higher weight and was assigned to K; the rest to sodium. Refinement, finally with anisotropic thermal parameters and a secondary extinction correction, converged at R = 2.5%. The larger residual peaks in the final difference Fourier map were 1.8 e/Å^3, 1.25 Å from In1, and −1.2 e/Å^3. The occupancies of the atoms did not deviate from unity by more than 2% (2σ) for In when the cations were held constant, and by more than 4% (2σ) for K and Na with In fixed, so all were held at full occupancy.

$Rb_3Na_{26}In_{48}$. The fact that the lattice parameters determined from powder data varied so slightly in the three compounds, ~0.066 Å over the range, produced some concern about whether the compounds were really ternary. In order to rule out any possiblity that they might be only binary, data were also collected on a larger single crystal of the Rb product. The structure was refined to final residuals R = 2.0, R_w = 2.5% with the Rb atoms occupying the K position in $K_3Na_{26}In_{48}$ (Table I). All sites were fully occupied to within 1.5σ. Later, some crystallites of the K and Rb compounds were checked by SEM/EDS and the compositions confirmed.

Physical Properties. Electric resistivity and magnetic susceptibility data were obtained for a single-phase sample of $K_3Na_{26}In_{48}$. The electrodeless "Q" method[14] was again used for the resistivity measurements on a powdered and sized sample mixed with chromatographic Al_2O_3. Data were taken every 10 deg over the 160–295 K range. The magnetization of a 25-mg sample was measured at a field of 3 T over 6–295 K on a Quantum Design MPMS SQUID magnetometer. The techniques for the measurements and the sample holder are described elsewhere.[6]

Results and Discussion

Structure Description. The final positional and isotropic-equivalent displacement parameters for the isostructural $K_3Na_{26}In_{48}$ and $Rb_3Na_{26}In_{48}$ are reported in Table II, and important distances are listed in Table III. A partial view of the unit cell is shown in Figure 1 with only In–In distances less than 3.5 Å drawn. The seemingly complex structure is in fact a three-dimensional network built of only two different In_{12} building blocks: arachno 12-vertex polyhedra ("drums") and closo icosahedra, each of which are shown isolated in Figure 2. Every vertex is bonded to another cluster via an exo In–In intercluster bond, this being, as usual, somewhat shorter than In–In distances within the clusters where delocalized bonding is operative.

The cluster arrangement shown in Figure 1 is in fact simple and well-known. Each icosahedron is, naturally, icosahedrally bonded to 12 separate *arachno*-In_{12} clusters (Figure 2). Each of the latter "drums" is surrounded by and bonded to four closo and eight arachno clusters to form a larger hexagonal antiprism. Two additional arachno units formally cap this antiprism to generate the chains, but these are not directly bonded to the central one. The structure is seen to consist of three nonintersecting chains of arachno clusters that lie in the middle of all faces of the cube and parallel to the different cell edges. These are interconnected to each other where they overlap (but do not interact), e.g., around 1, $^1/_2$, $^3/_4$ in Figure 1. (Note that the horizontal chain lying in the front face of the cube has been omitted.) All six chains that are so placed in the unit cell are also bonded to the closo icosahedra

Table II. Positional and Isotropic Equivalent Displacement Parameters for $A_3Na_{26}In_{48}$

atom	position	x	y	z	B_{eq},[a] Å^2
		$K_3Na_{26}In_{48}$			
In1	24 k	0	0.16357(7)	0.31861(7)	2.01(5)
In2	24 k	0	0.09176(7)	0.15237(7)	2.26(5)
In3	48 l	0.33289(5)	0.33010(5)	0.09488(4)	1.81(4)
K	6 b	0	$^1/_2$	$^1/_2$	2.5(3)
Na1	6 c	$^1/_4$	0	$^1/_2$	1.5(3)
Na2	6 d	$^1/_4$	$^1/_2$	0	2.8(4)
Na3	16 i	0.1892(3)	x	x	2.27(4)
Na4	24 k	0	0.2958(4)	0.1356(4)	2.6(3)
		$Rb_3Na_{26}In_{48}$			
In1	24 k	0	0.16415(3)	0.31863(3)	1.76(2)
In2	24 k	0	0.09257(3)	0.15348(3)	1.67(2)
In3	48 l	0.33314(2)	0.32961(2)	0.09512(2)	1.69(2)
Rb	6 b	0	$^1/_2$	$^1/_2$	1.89(5)
Na1	6 c	$^1/_4$	0	$^1/_2$	1.9(1)
Na2	6 d	$^1/_4$	$^1/_2$	0	2.1(1)
Na3	16 i	0.1898(1)	x	x	2.43(5)
Na4	24 k	0	0.2961(2)	0.1349(2)	2.4(1)

[a] $B_{eq} = (8\pi^2/3)\Sigma_i\Sigma_j U_{ij} a_i^* a_j^* \vec{a}_i \vec{a}_j$.

Table III. Distances of Nearest Neighbors about Each Atom in $A_3Na_{26}In_{48}$ (A = K, Rb)

atom 1	atom 2	K_3Na_{26}-In_{48}	Rb_3Na_{26}-In_{48}	atom 1	atom 2	K_3Na_{26}-In_{48}	Rb_3Na_{26}-In_{48}
In1	In2	2.909(2)	2.8981(7)	A	4 In1	3.924(1)	3.9386(5)
	2 In3	3.0633(9)	3.0751(4)		8 In3	4.1205(8)	4.1340(4)
	2 In3	3.123(1)	3.1274(6)		2 Na1	4.0160(1)	4.0252(3)
	A	3.924(1)	3.9386(5)		2 Na2	4.0160(1)	4.0252(3)
	Na2	3.228(1)	3.2308(5)		4 Na4	3.938(6)	3.936(3)
	2 Na3	3.706(2)	3.7163(8)				
	2 Na4	3.433(4)	3.440(2)	Na1	8 In3	3.3443(7)	3.3476(4)
	Na4	3.627(7)	3.643(3)		2 A	4.0160(1)	4.0252(3)
					4 Na4	3.760(6)	3.770(3)
In2	In1	2.909(2)	2.8981(7)				
	In2	2.948(2)	2.981(1)	Na2	4 In1	3.228(1)	3.2308(5)
	4 In2	3.019(1)	3.0480(6)		8 In3	3.3978(7)	3.4153(4)
	2 Na3	3.471(6)	3.482(3)		2 A	4.0160(1)	4.0252(3)
	Na4	3.289(6)	3.291(3)				
	2 Na4	3.497(6)	3.495(3)	Na3	3 In1	3.706(2)	3.7163(8)
					3 In2	3.471(6)	3.482(3)
In3	In1	3.0633(9)	3.0751(4)		3 In3	3.500(3)	3.497(2)
	In1	3.123(1)	3.1274(6)		3 In3	3.570(4)	3.567(2)
	In3	3.048(1)	3.0398(7)		Na1	3.38(1)	3.360(7)
	In3	3.052(2)	3.0632(7)		3 Na4	3.594(4)	3.613(2)
	In3	3.162(2)	3.1788(7)				
	A	4.1205(8)	4.1340(4)	Na4	2 In1	3.433(4)	3.440(2)
	Na1	3.3343(7)	3.3476(4)		In1	3.627(7)	3.643(3)
	Na2	3.3978(7)	3.4153(4)		In2	3.289(6)	3.291(3)
	Na3	3.500(3)	3.497(2)		2 In2	3.497(6)	3.495(3)
	Na3	3.570(4)	3.567(2)		2 In3	3.255(4)	3.257(2)
	Na4	3.255(4)	3.257(2)		2 In3	3.527(6)	3.540(3)
	Na4	3.527(6)	3.540(3)		A	3.938(6)	3.936(3)
					Na1	3.760(6)	3.770(3)
					2 Na3	3.594(4)	3.613(2)

(14) Shinar, J.; Dehner, B.; Beaudry, B. J.; Peterson, D. T. *Phys. Rev.* **1988**, *37B*, 2066.

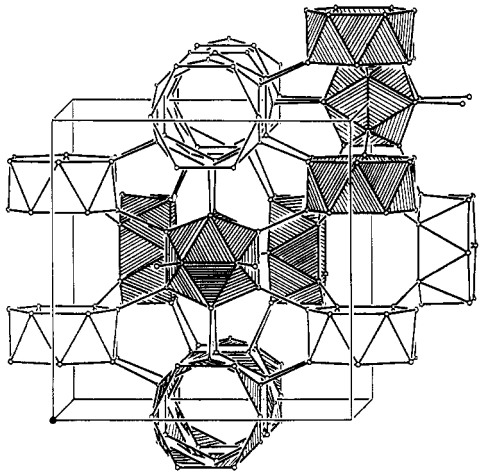

Figure 1. Portion of the indium network in the structure of $A_3Na_{26}In_{48}$. Some of the polyhedra are shaded to emphasize the building blocks: *closo*-In_{12} icosahedra and *arachno*-In_{12} hexagonal antisprisms (drums). Arachno clusters are connected via other clusters into chains lying in all faces of the cube, but the chain across the front face is not shown. The A atoms are centered in the larger cavity at 1, $^1/_2$, $^1/_2$ between arachno clusters in the same chain.

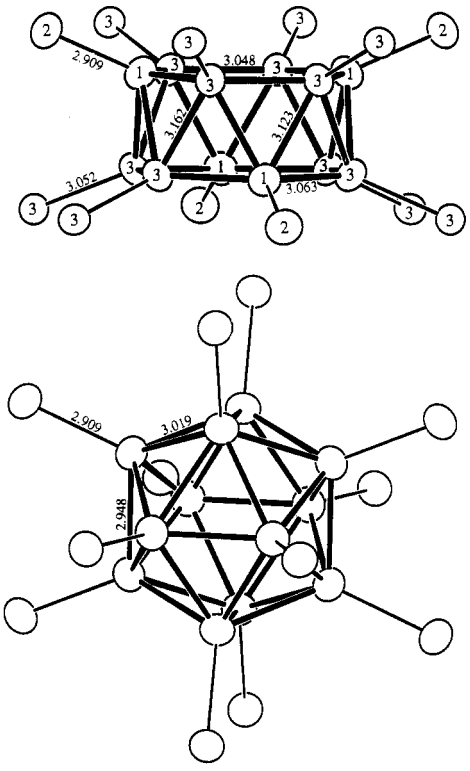

Figure 2. Separate *arachno*-In_{12} (top) and *closo*-In_{12} (bottom) cluster units with independent distances and the numbering system (94% probability thermal ellipsoids). All cluster atoms in the latter are In2.

that lie at the body center and at the corners of the cell. The structure is isotypic with the A15 (Cr_3Si or W_3O) type structure[15] *if* we equate metal atoms with the arachno groups and the nonmetals with closo icosahedra.

The *arachno*-In_{12} (In1, In3) cluster has D_{2d} ($\bar{4}m2$) point group symmetry but is close to D_{6d} symmetry (Figure 2, top). This polyhedron appears to be the first example of an arachno derivative of a 14-vertex closo species that would result from capping the two hexagonal faces of the observed cluster. The unknown *closo*-In_{14} cluster has 24 triangular faces and could be called an icositetrahedron (24-hedron). The hexagons that make up the arachno unit are not exactly planar, the In1 atoms in each being 0.056(3) Å (K) or 0.044(2) Å (Rb) outside the plane defined by the four In3 atoms. The distances around the hexagons also differ slightly, 3.048(1) (In3–In3) vs 3.063(1) Å (In1–In3) for K and 3.0398(7) vs 3.0751(4) Å for Rb derivatives. This combined with the out-of-plane displacement leads to ~126° angles at In1 and ~125° at In3. The distances between members of adjoining hexagons in a single drum are longer than those within them by 0.06–0.1 Å. This difference is probably caused by the lack of capping atoms on the rings, similar shortening of distances in open faces having been observed in other nido and arachno clusters.[6,7,10] Each of the In1 atoms lies trans to one another in each hexagon and is exo-bonded to an icosahedron, while each In3 atom is bonded to another *arachno*-In_{12} polyhedron in a separate, perpendicular chain. The arachno clusters are centered by the Na2 ions.

The closo icosahedra have the rare T_h point group symmetry and are built of In2 atoms only. There are two different bond distances; the six edges parallel to the unit cell axes (Figure 2, bottom) are shorter than the remaining fourteen: 2.948(2) vs 3.019(1) Å (K) and 2.981 vs 3.0480(6) Å (Rb). The vertices in each icosahedron are bonded to 12 different *arachno*-In_{12} polyhedra and thus also serve to interlink the chains. The distance differences within the *closo*-In_{12} clusters with K vs Rb are greater than elsewhere even though these cations are not nearest neighbors to this unit, doubtlessly reflecting packing requirements of the networks. Other examples of the T_h symmetry for 12-atom polyhedra are $(Al,Zn)_{12}$ units in $Mg_{11}Zn_{11}Al_6$,[16] zinc-centered Zn_{12} units in Mg_2Zn_{11}[17] and $NaZn_{13}$,[18] centered $Al_{12}W$ groups in WAl_{12},[19] and Ga_{12} polyhedra in $Li_{13}Cu_6Ga_{21}$.[20]

The cations are not shown in the figure, and generalities are sufficient to analyze these. All sodium atoms except Na2 cap triangular faces of the polyhedra. The Na2 and K (Rb) cations alternate along the cylindrical chains of arachno clusters, with Na2 lying within these and K (Rb, Cs) between them and centered on the cell faces (1, $^1/_2$, $^1/_2$, etc.). These A ions also alternate with Na1 ions at 1, $^1/_4$, $^3/_4$, etc. in cation chains that run in a perpendicular direction. The size of cavity about Na2 within the drum is not particularly distinctive relative to those containing the other types of sodium whereas the A site between them is 0.60 Å larger. These features are doubtlessly what limit this structure to the $Na_{26}A_3$ proportion with A = K, Rb, or Cs. Continued substitution of potassium for sodium does not fill the next larger site (Na3, 0.17 Å larger) but rather produces a series of three closely related structures.[10] The first is rhombohedral K_x-$Na_{22-x}Ga_{39}$ ($\sim 6 < x < \sim 12$) (analogous to Na_7Ga_{13}[21]) with two of the nine cation sites mixed, the second is partially ordered orthorhombic $K_xNa_{23-x}Ga_{39}$ ($\sim 16 < x < \sim 20$) structured like $Na_{22}Ga_{39}$,[22] and finally, thombohedral $K_{22}In_{39}$ reappears with a single type of cation.

Properties. The resistivity of $K_3Na_{26}In_{48}$ is linear with temperature over the range 160–295 K with a coefficient of +0.13%/deg and $\rho_{295} \sim 23$ $\mu\Omega$ cm. Such a resistivity is characteristic of a typical metal (21 $\mu\Omega$ cm for lead, for example[23]).

The magnetic susceptibilities of $K_3Na_{26}In_{48}$ over the 6–295 K range were temperature-independent and, after holder corrections, fell in the ranges of $-(13.40–14.42) \times 10^{-4}$ emu/mol. As before,[5,6] two types of diamagnetic corrections may be applied to these

(15) Hyde, B. G.; Andersson, S. *Inorganic Crystal Structures*; John Wiley and Sons: New York, 1989; p 330.
(16) Bergman, C.; Waugh, J. L. T.; Pauling, L. *Acta Crystallogr.* **1957**, *10*, 254.
(17) Samson, S. *Acta Chem. Scand.* **1949**, *3*, 835.
(18) Shoemaker, D. P.; Marsh, R. E.; Ewing, F. J.; Pauling, L. *Acta Crystallogr.* **1952**, *5*, 637.
(19) Adam, J.; Rich, J. B. *Acta Crystallogr.* **1954**, *7*, 813.
(20) Tillard-Charbonnel, M.; Belin, C. *J. Solid State Chem.* **1991**, *90*, 270.
(21) Frank-Cordier, U.; Cordier, G.; Schäfer, H. *Z. Naturforsch.* **1982**, *37B*, 119.
(22) Ling, R. G.; Belin, C. *Acta Crystallogr.* **1982**, *B38*, 1101.
(23) *Handbook of Chemistry and Physics*, 65th ed.; CRC Press: Boca Raton, FL, 1985; p F-120.

numbers. The first one, for the ion cores of the constituent elements, totals -10.81×10^{-4} emu/mol. The second correction is for the Larmor precession of the electron pairs in the cluster orbitals. We estimate 2.14 Å for the average orbital radius in *closo*-In_{12} and 2.96 Å for that in *arachno*-In_{12}, which give -3.36×10^{-4} and -7.42×10^{-4} emu/(mol cluster), respectively. According to the proportion of each cluster per formula unit, the total correction becomes $\chi_L = [1 \times 3.36 + 3 \times 7.42)] \times 10^{-4} = -25.62 \times 10^{-4}$ emu/mol. Combination of these and the measured susceptibilities provies $\chi_M = +(2.2\text{–}2.3) \times 10^{-3}$ emu/mol for $K_3Na_{26}In_{48}$. This result is typical for a moderate Pauli-type paramagnetism and is consistent with both the measured metal-like conductivity and the electron count based on theory (below).

Electronic Structure and Electron Count. Extended Hückel calculations were performed on the separate 12-bonded *closo*-In_{12} and *arachno*-In_{12} clusters. The procedure is described elsewhere.[6,24] These confirmed the expected (Wade's rule) $n + 1$ and $n + 3$ skeletal bonding orbitals in the respective closo and arachno species. Combination of these with the number of two-electron exo bonds for each cluster leads to local charges of -2 for the *closo*-In_{12} and -6 for *arachno*-In_{12}. Rough HOMO–LUMO gaps in each cluster are 3.7 and 1.9 eV, respectively. A band calculation for the anion network was not pursued.

The electron count for $K_3Na_{26}In_{48}$ can be done in the following way. Each unit cell contains two 12-bonded *closo*-In_{12} clusters, which require 26 skeletal and 12 exo-bond electrons each, and six 12-bonded *arachmo*-In_{12} clusters, which need 30 skeletal and 12 exo-bond electrons each. The total number of valence electrons becomes $2 \times (26 + 12) + 6 \times (30 + 12) = 328$. Since each In atom provides three valence electrons and each alkali metal atom one valence electron, the number of available electrons is $2 \times (3 + 26 + 48 \times 3) = 346$. This means that the compound is electron-rich with 18 (5.5%) extra electrons per unit cell. These are presumably delocalized in a conduction band, consistent with the observed metallic properties (above).

This novel structure once again illustrates the driving force for covalent bonding that is present in the anionic compounds of indium, both when delocalized in cluster units and in what can be described as simple two-center bonds between them. Many cluster types appear possible in these network structures beyond *closo*-In_{12}, *nido*-In_{11}, *arachno*-In_{10}, including octahedra, and *closo*-In_{16} units and the present *arachno*-In_{12} cluster. Even more examples can be captured when heteroatoms are used to alter the electronic requirements.[5,9,10] The structural variety and complexity of these solids arise from the problems of fitting clusters and spacers into ordered, space-filling, three-dimensional arrays with sufficient room for cations, while at the same time responding to an evidently strong electronic tendency to approach (or achieve) closed-shell, semiconducting configurations.

Acknowledgment. We are indebted to J. Shinar for the use of the "Q" resistivity apparatus and J. E. Ostenson for the measurement of the magnetic data.

Supplementary Material Available: Tables of data collection and refinement details and of anisotropic displacement parameters for $A_3Na_{26}In_{48}$ (A = K, Rb) (2 pages). Ordering information is given on any current masthead page.

(24) Hoffman, R. *J. Chem. Phys.* **1963**, *39*, 1397.